Bioorganic Chemistry 92 (2019) 103251

Contents lists available at ScienceDirect

Bioorganic Chemistry

journal homepage: www.elsevier.com/locate/bioorg

Design and synthesis of novel pyridazinoquinazoline derivatives as potent VEGFR-2 inhibitors: *In vitro* and *in vivo* study

Marwa G. El-Gazzar, Rania M. El-Hazek, Nashwa H. Zaher*, Mona A. El-Ghazaly

Department of Drug Radiation Research, National Center for Radiation Research and Technology (NCRRT), Egyptian Atomic Energy Authority (EAEA), PO Box 29, Nasr City, Cairo 11765, Egypt

ARTICLE INFO

Keywords:
Pyridazinoquinazoline
HCC
VEGFR-2 inhibitors
Caspase
Docking
Radiation

ABSTRACT

Worldwide, Hepatocellular Carcinoma (HCC) endures to be a prominent cause of cancer death. Treatment of HCC follows multiple therapies which are not entirely applicable for treatment of all patients. HCC usually arises contextual to chronic liver diseases and is often discovered at later stages which makes treatment options more complex. The present study aimed at design, synthesis & evaluation of new pyridazinoquinazoline derivatives as potential nontoxic anti-hepatocellular carcinoma (HCC) agents, through inhibition of Vascular endothelial growth factor -2 (VEGFR-2). Novel Pyridazino[3, 4, 5-*de*]quinazoline derivatives **(2-6)** were designed & synthesized. Their structures were confirmed via spectral and microanalytical data. They were tested for their *in vitro* VEGFR-2 inhibition & anticancer activity against human liver cancer cell line (HEPG-2). Molecular docking was investigated into VEGFR-2 site. *In vivo* studies of VEGRF-2 inhibition and the anti-apoptotic effect of the new compounds were determined in liver of irradiated rats. Toxicity of synthesized compounds was also assessed. The results showed that compounds **3-6** have significant antitumor activity and proved to be non-toxic. The ethoxy aniline derivative **6**, exhibited the highest activity both *in vitro* and *in vivo* compared to the reference drug used, sorafenib. Compound **6** could be considered a promising nontoxic anti HCC agent and this could be partially attributed to its VEGFR-2 inhibition. Future preclinical investigation would be carried out to confirm the specific and exact mechanism of action of these derivatives especially compound **6** as an effective pharmaceutical agent after full toxicological and pharmacological assessment.

1. Introduction

Globally, Hepatocellular Carcinoma (HCC), the destructive and invasive malignancy, is the second leading cause of cancer-related mortalities [1]. HCC incidence will continue rising in the future century, and unfortunately mortality remains high for most of patients [2]. At present, limited treatment regimens are available for this challenging disease. HCC treatment landscape is rising in complexity. The biggest challenge is that up to 80–90% of HCC patients suffers also liver cirrhosis due to different etiologies. Another challenge is the unexpected response toward different treatments. Currently, there is a necessity for refining treatment options for HCC patients [3]. Radiation therapy (RT) is adopted as one of the main modalities for cancer treatment. Historically, RT was regarded as ineffective treatment tool in HCC because of the of RT dose limitation. This is attributed to the sensitivity of surrounding non-malignant liver parenchyma toward radiation, leading to limited RT techniques [4]. Beside RT, chemotherapy constitutes one of the modalities of cancer treatment, either alone or in conjunction with other treatment regimens. Angiogenesis inhibitors have become important agents in treatment of HCC patients [5]. Nowadays, vascular endothelial growth factor (VEGF) is a crucial angiogenic factor expressed in tumors of all types of cancer analyzed. Putting this in consideration, researchers were encouraged for exploring the potential role of VEGF in immune modulation, and its role in combating most cancer types. [6]. Extensive studies on VEGF and its receptors over the past 10 years have revealed that this system is a major regulator for angiogenesis. VEGF has been reported to act as a survival factor for several tumor cells as well as normal cells by protecting against apoptosis-inducing treatments, such as chemotherapy and irradiation [7]. These treatments induce apoptosis through Caspase-3 expression, the main key component of apoptosis, which is responsible for the proteolytic cleavage of many crucial proteins. On the contrary, if a cell is not capable of undergoing apoptosis because of a mutation or a biochemical inhibition, it can continue dividing and develops to become a tumor [8].

Sorafenib (Nexavar) ® (4-[4-[[4-chloro-3-(trifluoromethyl) phenyl]

* Corresponding author.
E-mail address: nashwazah@hotmail.com (N.H. Zaher).

https://doi.org/10.1016/j.bioorg.2019.103251
Received 9 May 2019; Received in revised form 31 August 2019; Accepted 3 September 2019
Available online 09 September 2019

carbamoylamino] phenoxy]-*N*-methyl-pyridine-2-carboxamide), the 1st line oral treatment in advanced HCC. It was approved as antiangiogenic chemotherapeutic drug targeting tyrosine kinase receptor [9]. Besides, Kim and coworkers explored sorafenib mechanism of action through inhibition of VEGFR-2, VEGFR-3, and platelet-derived growth factor receptor-B activities [10]. However, sorafenib is not widely prescribed as it is expensive drug, not potent for treating metastasis cases, and expression of severe adverse side-effects, cardiovascular of which could be fatal [11]. Although, the prognosis of advanced HCC patients with early stage liver disease, was improved upon use of sorafenib, limited survival benefits were reported due to drug resistance and low response rates [12]. Bayer has developed regorafenib (Stivarga) ®. It is developed by adding a fluorine atom in the centered phenyl ring of sorafenib. It is prescribed for HCC patients whose disease progressed while treated with sorafenib. It was approved by US food & drug administration on April 27, 2017 [13] for use as second line treatment in HCC [14]. It provided survival benefit over sorafenib use, but unfortunately, serious side effects were reported [15].

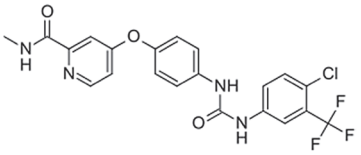

Sorafenib

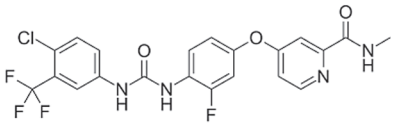

Regorafenib

Other chemically related compounds were investigated as second line HCC treatment (Fig. 1), but reported to be non-significantly potent to Sorafenib at the same time didn't show better therapeutic index. Some of them reported inferior potency and more severe toxicity to sorafinib as sunitinib [16]. While, brivanib, erlotinib & tivantinib did not significantly improve overall survival in advanced HCC patients treated previously with sorafenib [17–19]. Linifanib was also investigated but studies favored sorafenib in safety [20]. Subsequently, clinical trials of all above mentioned compounds were stopped.

In recent decades, 1,4-disubstituted phathalazine moiety emerged as promising scaffold as potent VEGFR-2 inhibitor and anticancer agent [21]. Accordingly extensive investigations have been carried out for designing and synthesizing of different molecules comprising phathalazine as potential VEGFR-2 inhibitors, but unfortunately no approved drug has been marketed clinically for use till now.

Vatalanib, a 1-anilino-4-substituted phthalazineamine based structure was developed as specific VEGFR-2 inhibitor for colorectal cancer treatment. It was discontinued in phase III clinical investigations. Valatanib failed to reveal any clinical benefit for patients suffering metastatic colorectal cancer and didn't improve the overall survival for them, besides emerged side effects as hypertension, hyperlipidemia and nausea were reported [22]. Behalo and coworkers reported recently some new phthalazine based molecules as potential anticancer agents against human cancer cell lines [23].

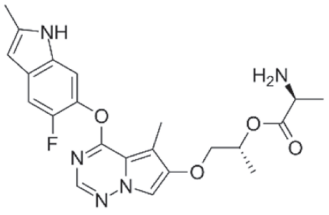

Brivanib

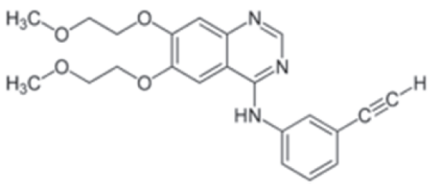

Erlotinib

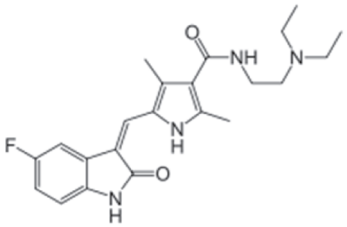

Sunitinib

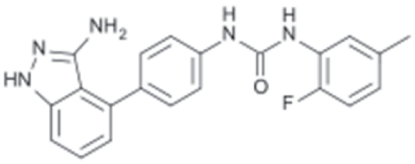

Linifanib

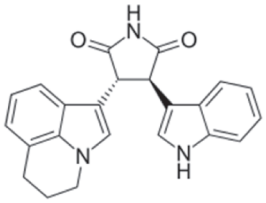

Tivantinib

Fig. 1. Structure of compounds evaluated and failed as second line HCC treatment.

Luminol (5-amino-2,3-dihydrophthalazine-1,4-dione), a bifunctional phthalazine reactive precursor-based molecule. It is a chemical exhibiting chemiluminescence. It is commonly used in forensics as a diagnostic tool for the detection of blood stains [24].

Fused pyrimidine with phthalazine yields pyridazinoquinazoline tricyclic molecule. Fused pyridazinoquinazoline is a well-known moiety for its diverse biological activities. Some derivatives were reported recently by Vaseghi and coworkers [25], for their anticancer activity on Melanoma and Prostate Cell Lines. Interestingly pyridazinoquinazoline, was not investigated as anti HCC via VEGFR-2 inhibition.

Based on all the previous findings, and as continuation of our previous work aimed at synthesizing novel promising anticancer agents [26,27], we were inspired to design and synthesize a novel series of Pyridazino[3, 4, 5-*de*]quinazoline derivatives starting from Luminol with the prime aim of developing agents targeting VEGFR-2 with potential anticancer activity towards hepatocellular carcinoma cells (HepG2), by performing *in vitro*, *in vivo* inhibitory evaluation, molecular docking study and acute toxicity assessment.

1.1. Rationale and design

Vatalanib (N-(4-chlorophenyl)-4-(pyridin-4-ylmethyl)phthalazin- 1-amine), is an oral angiogenesis inhibitor being developed by Schering (in collaboration with Novartis), used for solid tumors treatment in metastatic colon cancer and non-small cell lung cancer (NSCLC) [28]. Vatalanib inhibits crucial angiogenesis enzymes involved in tumor growth and metastasis. The following three tyrosine kinase domains; vascular endothelial growth factor (VEGF) receptors, platelet-derived growth factor (PDGF) receptor and c-kit were reported as target sites into which vatalanib selectively bound [29]. Many attempts in medicinal chemistry were performed to produce novel tyrosine kinase inhibitors by designing tricyclic compounds or ring addition to stabilize the structure of known scaffolds. These attempts led to promising and potent derivatives by providing additional binding within the target enzymes [30–33].

Inspired by these facts, and due to our interest in the treatment of liver cancer being the second cause of cancer mortality worldwide, we decided to perform structural modifications on vatalanib by introducing a third ring on phthalazine main scaffold aiming to obtain a more rigid structure that could increase binding affinity to the essential amino acids into VEGFR2 active binding site of (Fig. 2). Moreover, varying p-substitutions on the aniline moiety will result in various binding interactions within the hydrophobic back pocket leading to different inhibitory activity.

2. Materials and methods

2.1. Chemistry

2.1.1. General

A Stuart melting point apparatus (Stuart Scientific, Redhill, UK) was used for recording of uncorrected melting points and were carried in open capillary tubes. FTIR Shimadzu spectrometer (Shimadzu, Tokyo, Japan) was used for recording Infrared (IR) spectra of the compounds. A Varian Mercury Plus Oxford (400 MHz for ^{1}H NMR and 100 MHz for ^{13}C NMR) spectrometer (Varian Inc., Palo Alto, CA) was used for recording ^{1}H NMR and ^{13}C NMR spectra, using TMS as an internal Standard and DMSO-d_6 as solvent. Mass spectra were run on HP Model MS-5988 (Hewlett Packard, Palo, Alto, California, USA). A Carlo Erba 1108 Elemental Analyzer (Heraeus, Hanau, Germany), was used for obtaining microanalyses values. Pre-coated SiO2 gel (HF254, 200 mesh) aluminum plates (Merk, Darmstadt, Germany) were used as TLC for checking of reactions' Completion, where a developing solvent system of chloroform/methanol (7:3) was used and the spots were visualized under UV light. IR, ^{1}H NMR, ^{13}C NMR, Mass and elemental analysis were consistent with the assigned structures. All reagents used were purchased from Sigma (St. Louis, MO) of analytical grade.

9-benzyl-3-chloro-7H-pyridazino[3,4,5-*de*]quinazoline-8(9H)-thione **(2)**

An equimolar concentration of compound 1 [27] and benzyl isothiocyanate was refluxed in ethanol for 4 h. The solvent was removed under reduced pressure. The precipitate formed was washed with diethyl ether, dried and recrystallized from dioxane to afford compound 2 Yield, 81%; m.p.; 198–199 °C; IR (KBr, cm^{-1}): 3287 (NH), 3088 (CH arom.), 2945, 2839 (CH aliph.), 1570 (C=S). MS (*m/z*): 326 (M+, 15.65%), 129 (100% base peak). ^{1}H NMR (DMSO-d_6, δ, ppm): 5.25 (s, 2H, CH2 benzyl), 7.18–7.26 (m, 5H, Ar−H), 7.62–7.75 (m, 3H, Ar−H), 8.11 (s, 1H, NH, D_2O exch.). ^{13}C NMR (DMSO-d_6, δ, ppm): 53.68 (CH_2 benzyl), 117.29, 126.35, 126.68, 126.8, 127.97 (2), 128.43, 128.59 (2), 128.92, 136.74, 141.71, 150.08, 153.92, 177.16 (C=S). MS (*m/z*): 326 (M+, 15.78%), 129 (100%). Analysis calculated for: $C_{16}H_{11}ClN_4S$ (326.04): C, 58.81; H, 3.39; Cl, 10.85; N, 17.14; S, 9.81; found: C, 58.98; H, 3.43; Cl, 10.91; N, 17.09; S, 10.03.

2.1.2. General procedure for the synthesis of compounds 3-6

An equimolar concentration of compound 2 and each of the corresponding aromatic amine p-fluoroaniline p-chloroaniline, p-methoxyaniline and p-ethoxyaniline, was refluxed in ethanol for 4 h. The solvent was removed under reduced pressure. The precipitate formed was washed with diethyl ether, dried and recrystallized from dioxane to afford compounds **3–6**, respectively.

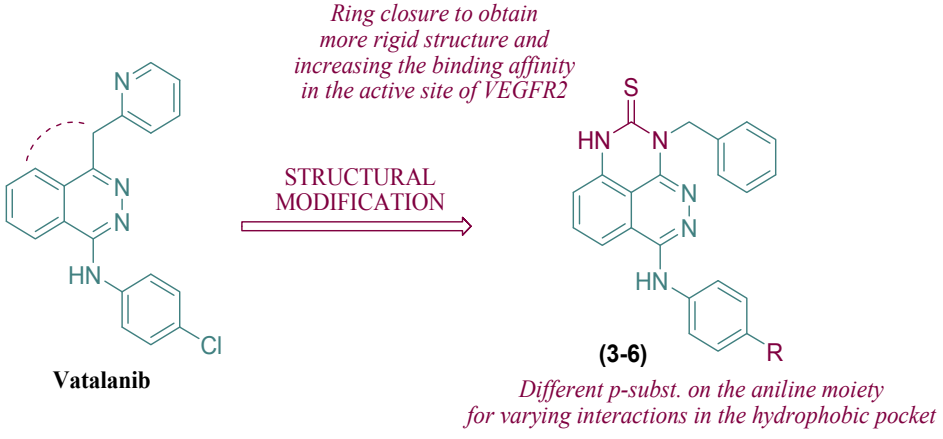

Fig. 2. Design of target compounds based on the lead compound vatalanib.

2.1.2.1. 9-benzyl-3-((4-fluorophenyl)amino)-7H-pyridazino[3,4,5-de] quinazoline-8(9H)-thione ***(3)***. Yield % 80; m.p.; > 280 °C; IR (KBr, cm^{-1}): 3291, 3282 (2NH), 3100 (CH arom.), 2940, 2833 (CH aliph.),1572 (C═S); ^{1}H NMR (DMSO-d_6, δ, ppm): 5.24 (s, 2H, CH_2 benzyl), 7.14–7.26 (m, 5H, Ar−H), 7.81–7.96 (m, 3H, Ar−H), 7.82, 7.83 (d, 2H, Ar−H, J = 8.0 Hz), 7.89, 7.91 (d, 2H, Ar−H, J = 8.0 Hz) 8.23, 8,85 (2 s, 2H, 2NH, D_2O exch.). ^{13}C NMR (DMSO-d_6, δ, ppm): 53.68 (CH_2 benzyl), 117.02 (2), 117.29, 118.72 (2), 120.58, 126.35, 126.68, 127.97 (2), 128.43, 128.59 (2), 128.92, 136.74, 139.52, 141.71, 153.92 (2), 160.46, 177.16 (C═S). MS (*m/z*): 401 (M^+, 24.32%), 91 (100%). Analysis calculated for: $C_{22}H_{16}FN_5S$ (401.46): C, 65.82; H, 4.02; F, 4.73; N, 17.44; S, 7.99; found: C, 65.97; H, 4.17; F, 4.59; N, 17.29; S, 7.76.

2.1.2.2. 9-benzyl-3-((4-chlorophenyl)amino)-7H-pyridazino[3,4,5-de] quinazoline-8(9H)-thione ***(4)***. Yield % 80; m.p.; > 280 °C; IR (KBr, cm^{-1}): 3267, 3242 (2NH), 3094 (CH arom.), 2938, 2828 (CH aliph.), 1567 (C═S), 567 (C−Cl). ^{1}H NMR (DMSO-d_6, δ, ppm): 5.24 (s, 2H, CH2 benzyl), 7.18–7.26 (m, 5H, Ar−H), 7.38, 7.41 (d, 2H, Ar−H, J = 8.0 Hz), 7.55, 7.57 (d, 2H, Ar−H, J = 8.0 Hz), 7.81–7.95 (m, 3H, Ar−H), 8.13, 8,82 (2 s, 2H, 2NH, D_2O exch.) ^{13}C NMR (DMSO-d_6, δ, ppm): 53.68 (CH_2 benzyl), 117.29, 119.81 (2), 120.58, 126.35, 126.68, 127.97 (2), 128.43, 128.59 (2), 128.92, 129.18, 129.88 (2), 136.74, 139.52, 141.71, 153.92 (2), 177.16 (C═S). MS (*m/z*): 417 (M^+, 24.32%), 91 (100%). Analysis calculated for $C_{22}H_{16}ClN_5S$ (417.92): C, 63.23; H, 3.86; Cl, 8.48; N, 16.76; S, 7.67; found: C, 63.41; H, 3.90; Cl, 8.25; N, 16.53; S, 7.59.

2.1.2.3. 9-benzyl-3-((4-methoxyphenyl)amino)-7H-pyridazino[3,4,5-de] quinazoline-8(9H)-thione ***(5)***. Yield % 82; m.p.; > 280 °C; IR (KBr, cm^{-1}): 3291, 3287 (2NH), 3067 (CH arom.), 2932, 2823 (CH aliph.), 1578 (C═S); ^{1}H NMR (DMSO-d_6, δ, ppm): 3.76 (s, 3H, OCH3), 5.24 (s, 2H, CH_2 benzyl), 6.59, 6.62 (d, 2H, Ar−H, J = 8.8 Hz), 6.99, 7.02 (d, 2H, Ar−H, J = 8.8 Hz), 7.18–7.26 (m, 5H, Ar−H), 7.81–7.95 (m, 3H, Ar−H), 8.33, 8,85 (2 s, 2H, 2NH, D_2O exch.). ^{13}C NMR (DMSO-d_6, δ, ppm): 53.68 (OCH3), 55.46 (CH2 benzyl), 114.42 (2), 117.29, 120.10 (2), 120.58, 126.35, 126.68, 127.97 (2), 128.43, 128.59 (2), 128.92, 136.74, 139.52, 141.71, 153.92 (2), 156.89, 177.16 (C═S). MS (*m/z*): 413 (M+, 18.95%), 122 (100%). Analysis calculated for $C_{23}H_{19}N_5OS$ (413.50): C, 66.81; H, 4.63; N, 16.94; O, 3.87; S, 7.75; found: C, 66.89; H, 4.70; N, 16.87; O, 3.69; S, 7.71.

2.1.2.4. 9-benzyl-3-((4-ethoxyphenyl)amino)-7H-pyridazino[3,4,5-de] quinazoline-8(9H)-thione ***(6)***. Yield % 85; m.p.; > 280 °C; IR (IR (KBr, cm^{-1}) cm^{-1}): 3298, 3224 (2NH), 3090 (CH arom.), 2945, 2812 (CH aliph.), 1577 (C═S), ^{1}H NMR (DMSO-d_6, δ, ppm): 1.21–1.25 (t, 3H, CH3, J = 7.2 Hz), 3.99–4.04 (q, 2H, CH_2, J = 7.2 Hz), 5.24 (s, 2H, CH_2 benzyl), 6.61, 6.63 (d, 2H, Ar−H, J = 8.8 Hz), 7.03, 7.05 (d, 2H, Ar−H, J = 8.8 Hz), 7.18–7.26 (m, 5H, Ar−H), 7.81–7.95 (m, 3H, Ar−H), 8.23, 8,75 (2 s, 2H, 2NH, D_2O exch.). ^{13}C NMR (DMSO-d_6, δ, ppm): 14.73 (OCH_2CH_3), 53.68 (CH_2 benzyl), 63.69 (OCH_2CH_3), 114.43 (2), 117.29, 120.10 (2), 120.58, 126.35, 126.68, 127.97 (2), 128.43, 128.59 (2), 128.92, 136.74, 139.52, 141.71, 153.92 (2), 156.19, 177.16 (C═S). MS (*m/z*): 427 (M+, 29.12%), 121 (100%). Analysis calculated for $C_{24}H_{21}N_5OS$ (427.53): C, 67.43; H, 4.95; N, 16.38; O, 3.74; S, 7.50; found: C, 67.51; H, 5.02; N, 16.27; O, 3.79; S, 7.56.

2.2. Biological evaluation

2.2.1. Animals

Male Wistar rats (150–180 g) were used for Enzyme-Linked Immunosorbent Assay (ELISA), whereas adult male swiss albino mice (25–35 g) were used for acute toxicity test. The animals were purchased from the animal breeding unit of the National Research Centre, Giza, Egypt, and acclimatized in the animal facility of the National Centre for Radiation Research and Technology (NCRRT), Atomic Energy Authority, Cairo, Egypt, for one week before being used. Animals were housed at a temperature of 25 ± 5 °C, humidity of 60 ± 5% and 12/12-h light-dark cycle. They were fed standard laboratory chow and water ad libitum. The study was conducted folloeing the guidelines set by the European Economic Community (EEC) regulations (Revised Directive 86/609/EEC)

2.2.2. Irradiation

Animals were exposed to whole body irradiation at an acute dose level of 6 Gy [34] at the NCRRT using the Gamma Cell-40 biological irradiator with a Caesium137 source (Atomic Energy of Canada Ltd; Sheridan Science and Technology Park, Mississauga, Ontario, Canada). The radiation dose rate was 0.46 Gy/min.

2.2.3. In-Vitro studies

2.2.3.1. Estimation of anti-cancer activity against HepG2 cell line using MTT assay. For monitoring *in vitro* cytotoxicity, the MTT method was used with multiwell plates. The entire synthesized compounds were prepared each in stock concentration of 10 mM in DMSO which was then used to prepare the working dilution. The final working concentration used in the experiments was ≤0.5% in DMSO. Human liver cancer cell line (HepG2) was cultured according to the manufacturer's instructions. The compounds in serial dilutions (0.01, 0.1, 1.0, 10 and 100 μM) were added after 24 h of culture and the cells were cultured for another 24 h at 37 °C. The cell viability was determined in each experiment using MTT (3-(4, 5-dimethylthiazol-2-yl)-2, 5-diphenyltetrazolium bromide) colorimetric assay. A microplate reader was utilized to measure the optical density at 540 nm. The experiment was conducted in triplicate. Data was calculated as cell viability percentage.

2.2.3.2. VEGFR-2 enzyme inhibition assay. VEGFR-2 kinase activity was measured by use of the RayBio Human VEGFR2 ELISA (Enzyme-Linked Immunosorbent Assay) kit according to manufacturer's instructions. The optical density was measured at 450 nm. The results were expressed as IC50 and presented in Table 1.

2.2.4. In-vivo studies

2.2.4.1. Experimental design. Rats were blindly allocated into seven groups, consisting of 8 rats each (n = 8). Group 1: served as control non-irradiated animals, Group 2: rats were irradiated at 6 Gy but left untreated, Group 3: rats were given sorafenib (60 mg/kg) as a reference drug, Group 4, 5, 6, 7: rats were given the newly synthesized compounds 3, 4, 5 and 6 respectively in a dose of (60 mg/kg) similar to the reference dose of Sorafenib [35]. All compounds were delivered orally after one hour of irradiation and treatment continued for 2 days further. On the third day, the rats were sacrificed by decapitation. The liver tissue was separated and stored at −80 °C in order to prepare later liver homogenates in appropriate media according to the parameters to be measured using a Glas Col®homogenizer (Terre Haute, IN, USA).

Table 1
In vitro Anticancer Activity against HepG2 Cell Line, *in vitro* VEGFR2 Inhibitory Activity and Docking Scores of the Synthesized Compounds.

Cpd. No.	IC50 (HEPG2) (μM)	IC50 (VEGFR2) (μM)	DockingScore (Kcal/mol)
1	20.8	–	−8.92
2	7.8	–	−13.12
3	0.68	0.21	−14.35
4	0.9	0.53	−14.41
5	0.82	0.43	−14.75
6	0.22	0.03	−15.21
Sorafenib	1.06	0.03	−17.45
Vatalinib	17.43	0.18	−17.12

2.2.4.2. VEGFR-2 enzyme inhibition assay. Liver homogenates were prepared in phosphate buffer saline PBS (pH 7.0–7.2). The homogenates were centrifuged for 5 min at 5000 × g. The supernatant was removed and assayed immediately for Vascular Endothelial Growth Factor Receptor 2 (VEGFR2) using ELISA Kit specific for rats according to manufacturer's instructions, obtained from Koma Biotech Inc., Korea. This assay depends on binding VEGFR2 antigen to a specific immobilized antibody. The formed immune complex binds to avidin-peroxidase conjugate, and a color developed in proportion to the amount of VEGFR2 bound. An ELISA plate reader set at 450 nm was used to measure the optical density of each sample. Values were expressed as ng/g tissue.

2.2.4.3. Caspase-3 activity. Measurement of liver caspase-3 activity was performed using ELISA Kit specific for rats (Axxora, Lorrach, Germany), which was performed according to the manufacturer's guidelines. An ELISA plate reader set at 450 nm was used to measure the optical density of each sample. Values were expressed as pg/g tissue.

2.2.4.4. Acute toxicity. The approximate 50% lethal dose (ALD50) of the compounds (3, 4, 5 and 6) was determined. Adult male Swiss albino mice (3–4 months) weighing 25–35 g were obtained from the animal breeding unit of the National Research Centre, Giza, Egypt.

A total of 40 mice were allocated into 5 groups (n = 8) in labeled cages. Compounds under investigation were injected intraperitoneally (i.p.) at different dose levels (30, 60, 100, 400 and 800 mg/kg. b.wt). Animals were kept under observation for 24–48 h during which any mortality in each group was recorded. After drug administration, all the animals had free access to food and water. The ALD50 was calculated from the data obtained, according to the method of Smith [36].

3. Statistical analysis

All data were expressed as mean values ± standard error of the mean (SEM). One-way analysis of variance (ANOVA) was used for statistical comparisons between different groups followed by Tukey-Kramer multiple comparison test. Probability values less than or equal to 0.05 ($P \leq 0.05$) were considered statistically significant.

4. Molecular docking

Molecular Operating Environment (MOE) software version 2014.0901, was used for performing the molecular docking studies. Structures of the synthesized compounds were drawn on MOE. Hamiltonian-Force Field-MMFF94x was used to minimize structures' energy. The force field partial charges were calculated for each compound. Default settings were utilized for analysis of conformational Stochastic of compounds. The most stable 4 conformers for each compound were retained. The X-ray crystal structure of VEGFR-2 in complex with sorafenib was downloaded from http://www.rscb.org/pdb (PDB ID: 4ASD). The protein-ligand complex obtained from the protein data bank (pdb) was prepared for docking as follows: 1-The enzyme was 3D protonated, then optimization of the system was done. 2- Chain B of the protein along with co-crystallized water molecules were deleted. 3-Determination and isolation of the binding pocket took place, then hiding the back bone. MOEDOCK was used to determine Flexible docking of ligand-rigid receptor of the most stable conformers. Scoring was performed using alpha triangle placement method and London dG as a function. Force field refinement was applied to the obtained poses using the same scoring function. Retaining thirty of the most stable docking models for each ligand with the best scored conformation was done. Sorafenib was re-docked into the active binding site of 4ASD for validation of the docking procedures. The validation results showed a near perfect alignment with the original ligand and displayed the same binding interactions as obtained from the X-ray crystallography pdb file with RMSD of 0.411 Å with docking score (S = −17.45 kcal/mol). Docking results are shown in Table 1.

5. Results & discussion

5.1. Chemistry

In this work, bifunctional luminol was used as a key precursor for the synthesis of novel pyridazino[3,4,5-*de*]quinazoline derivatives **(2–6)** which is outlined in Scheme 1. Structures of the newly obtained compounds were entirely investigated via spectral and microanalytical data, where results were in conformity with their postulated structures. First, chlorination of luminol with thionyl chloride in refluxing ethanol, afforded compound **1** [27]. We reported Compound **1** as the most potent among a series of phthalazine, against HEPG2 cell line [27]. It was then in our current research further cyclized to pyridazino[3,4,5-*de*] quinazoline **2** upon its reaction with benzyl isothiocyanate in refluxing ethanol. IR spectrum of compound **2** revealed a medium intensity band at 3287 cm^{-1} due to NH stretch, and a band at 3088 cm^{-1} ascribed for phenyl absorption. In addition to absorption band at 1570 cm^{-1} attributed to (C═S). ^{1}H NMR spectrum of compound **2**, showed absorption singlet signal at δ 5.25 ppm attributed to benzyl moiety, multiplet signals at range 7.18–7.75 ppm assigned for aromatic hydrogens. A deuterium exchangeable singlet signal with D_2O was displayed at 8.11 ppm for NH group, confirming cyclization to pyridazino quinazoline. ^{13}C NMR spectrum of compound **2** exhibited the most shielded carbon atom at absorption 53.68 ppm ascribed for (CH_2 benzyl), while the most deshieleded cabon atom of (C═S) was displayed at absorption 177.16 ppm. In addition to signals displayed at range 117.29–153.92 ppm, attributed to phenyl carbons.

To mimic the structure of the lead compound vatalanib, the chlorine group in compound **2** was used to introduce different aromatic amines to afford compounds **3–6** in a very good yield**,** perceiving main structural features of vatalanib as VEGRF-2 inhibitor **(**Fig. 2**)**. IR spectra of compounds **3-6** revealed extra NH band, such that both NH bands for each compound, were displayed at range 3224–3298 cm^{-1}. Moreover, ^{1}H NMR spectra of compounds **3-6** displayed two singlet signals exchangeable with deuterium at range 8.13–8.33 ppm & 8.82–8.85 ppm attributed for the 2 NH groups present. The benzyl protons were revealed as singlet signal at 5.24 ppm. Aromatic protons were exhibited as multiplet signals at range 7.10–7.83 ppm & 7.81–7.95 ppm for benzyl and pyridazino quinazoiline moieties, respectively. While AB system protons for the para substituted phenyl moiety were revealed as pair of doublet of doublet signals at range 6.59–7.91 ppm, confirming introduction of aromatic amine moieties at specified position. ^{1}H NMR spectrum of compound **5** revealed extra upfield singlet signal attributed to methoxy group introduced. While ^{1}H NMR spectrum of compound **6** displayed extra upfield triplet and quartet signals at 1.21–1.25 & 3.99–4.04 ppm, respectively ascribed for ethoxy protons introduced. ^{13}C NMR spectra of compound **3-6** revealed signal at 53.68 ppm for **C**H_2 benzyl. While the most downfield signal appeared at 177.16 ppm ascribed for **C**═S. In addition to aromatic carbons which were displayed at range 114.42–160.46 ppm. ^{13}C NMR spectrum of compound **5** displayed extra upfield signal at 53.68 ppm for the methoxy group introduced. While ^{13}C NMR spectrum of compound **6** showed extra 2 signals at 14.73 & 63.69 ppm attributed to CH_3 and CH_2, respectively of the ethoxy group introduced. Moreover, mass spectra and microanalytical data of compounds **2-6** were in agreement with their proposed structures as listed in details in the material and methods section.

It is of added interest to mention that the newly obtained compounds closely interpolating Lipiniski's Rule of Five.

5.2. Biological evaluation

In this study, we investigated anti-cancer efficacy and activity of novel Pyridazino[3, 4, 5-de] quinazoline derivatives against hepatocellular carcinoma (HCC) cells *in vitro*. The study was expanded into *in*

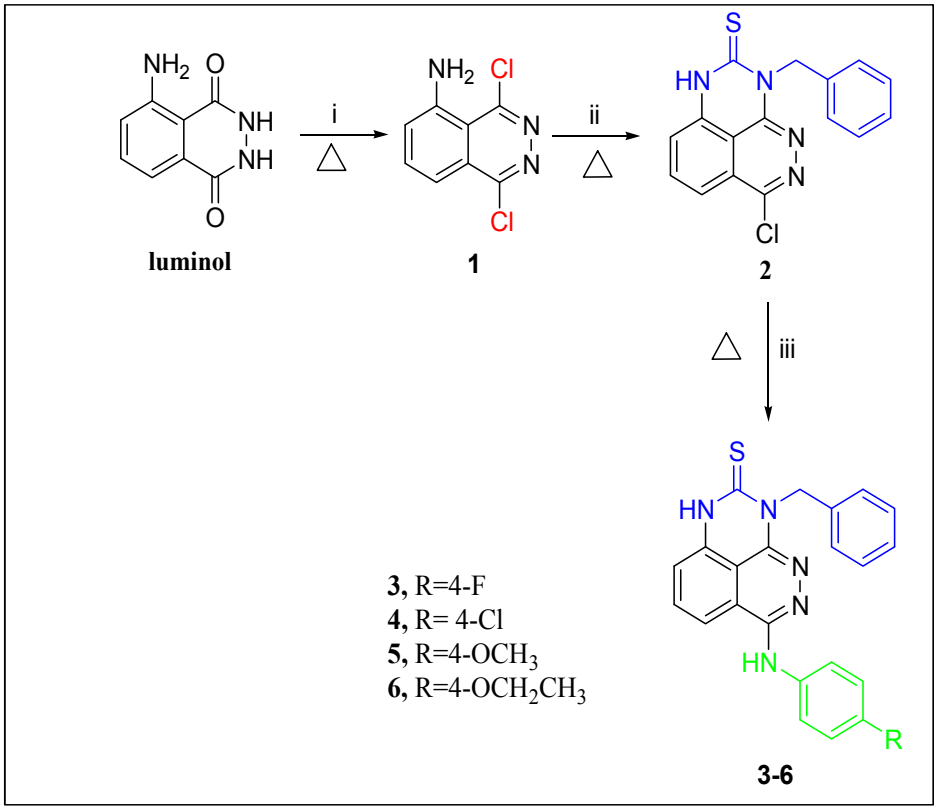

Scheme 1. Synthetic pathway for compounds 1-6. i; thionyl chloride, ethanol, ii; benzyl isothiocyanate, ethanol, iii; aromatic amine, ethanol.

vivo normal liver tissue of irradiated rats to study its possible effect on VEGFR-2 and their toxic effect on normal tissues when associated with radiation as an adjuvant therapy.

5.2.1. *In-vitro studies*

The newly synthesized compounds (2-6) were evaluated for their *in vitro* cytotoxic activity against HepG2 (Hepatocellular carcinoma) cell line by the MTT assay method. Sorafenib, the only systemic agent known to improve survival for hepatocellular carcinoma (HCC) [37], was used as a reference drug in this study. In order to obtain the survival curves of the cancer cell lines, the relationship between surviving fraction and drug concentration was plotted. Concentration required for 50% inhibition of cell viability (IC_{50}) was calculated, (Table 1). From the obtained results, it was obvious that most of the synthesized compounds displayed excellent anticancer activity against HepG2 cell line. In particular, compound 6 exhibited maximum cytotoxic activity against HepG2 cell line (IC50 = 0.22 μM) and is nearly 5 times more active than standard sorafenib (IC50 = 1.06 μM). The other Pyridazino [3, 4, 5-de] quinazoline derivatives (3-5) showed IC50 = 0.68, 0.9, 0.82 μM respectively, against HepG2 cell line (Table 1).

The newly prepared compounds **(2-6)** have been further assayed for their selectivity towards Sorafenib's crucial target, VEGFR2 indicated by IC50 values. The results were reported as a 50% inhibition concentration value (IC50, determined in triplicate) Table 1. The tested compounds 3-6 displayed good inhibitory activity with IC50 values ranging from 0.03 to 0.9 mM compared to sorafenib ((IC_{50} = 0.03 μM). The current study revealed that the most potent cytotoxic derivative is compound 6 since it might suppress angiogenesis by a decrease in the expression of VEGFR2 with IC50 = 0.03 μM which is equivalent to that of sorafenib (Table 1). VEGFR2-mediated activation of endothelial cells (ECs) is critical for angiogenesis. This is attributed to its capability to induce EC signaling pathways that regulate EC proliferation, migration, and survival, therefore, serves as an important role during tumor growth, invasion and metastasis. HCC and other tumors have been characterized by overexpression of VEGF, a crucial growth factor controlling angiogenesis, which has been associated with tumor progression, microvascular invasion, metastasis, and poor survival rate [38,39]. The VEGFR2 inhibitory activities of sorafenib had led to the inhibition of angiogenesis [40], which in turn is the possible mechanism of action for the newly synthetized compounds.

5.2.2. *In-vivo studies*

The second goal of this study was to investigate if the newly synthetized compounds show any inhibitory effect on VEGFR-2 as that of sorafenib *in vivo* as well as to find its possible toxic effect on normal liver tissue. Our rationale for utilizing ionizing radiation arises from its role in VEGFR2 activation. It is vital to maintain good liver function upon HCC management, for this, radiotherapy could not be adopted on wide basis. Therefore, if the newly synthetized compounds could guard against radiation-induced liver toxicity, there will be a promising approach to be used as adjuvant with radiotherapy.

It has been observed that radiation upsurges VEGF release from tumor cells in many types. Subsequently, the angiogenic response of the tissue may increase. This reaction is considered as self-protection for the tumor cells or a “survival mechanism” for damage caused by radiation [41]. Therefore, radiation may induce a protective role for tumor cells in the support of their associated vasculature that may be down-regulated by co-administration of angiogenesis inhibitors. This could rationalize the concurrent administration of angiogenesis inhibitors such as sorafenib and radiotherapy in cancer.

While sorafenib has rapidly become accepted as first-line treatment for locally advanced and metastatic HCC, the survival benefit remains modest at less than 3 months and sorafenib imparts no delay in time to symptomatic progression. At the same time not appropriate to all HCC patients [42]. Moreover, sorafenib has been proven to show drug resistance attributed to the hypoxic microenvironment of liver, which resulted in limited survival benefits because of low response rates [12].

All the tested compounds 3-6 were shown to be potent in-vitro

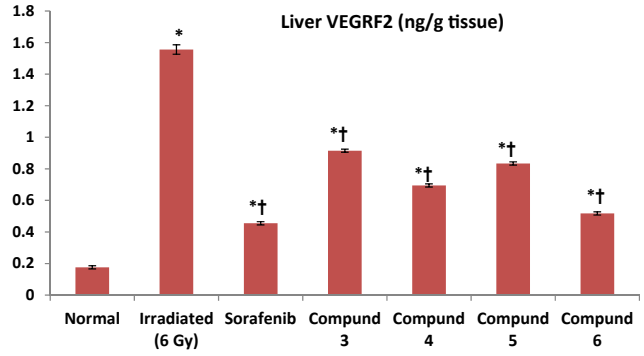

Fig. 3. Effect of Pyridazino[3, 4, 5-*de*]quinazoline Derivatives (3-6) and sorafenib, on expression of VEGFR2 in liver of irradiated rats. Values are plotted as means. *P ≤ 0.05 compared to normal, †P ≤ 0.05 compared to irradiated rats.

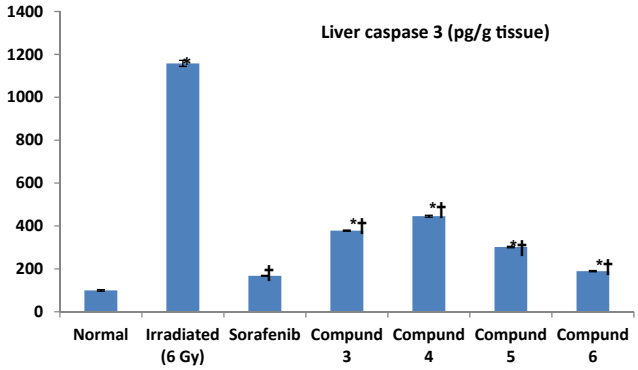

Fig. 4. Effect of Pyridazino[3, 4, 5-*de*]quinazoline Derivatives (3-6) and sorafenib, on liver caspase 3 of irradiated rats. Values are plotted as means. *P ≤ 0.05 compared to normal, †P ≤ 0.05 compared to irradiated rats.

VEGFR2 inhibitors. These compounds were subjected to in-vivo VEGFR2 inhibition assay using sorafenib as a reference standard drug. Exposure of rats to 6 Gy gamma radiation led to a dramatic increase in expression of VEGFR2 in liver tissue by 8 folds after 3 days (Fig. 3). This elevation in VEGFR2 expression after irradiation, is consistent with previous research reporting elevated level of VEGF after irradiation causing promoted hepatoma cell growth and enhanced intra tumor angiogenesis and hence increased invasiveness [43]. Improved outcomes were reported in preclinical studies through synergistic antitumor activity as a result of the combination of VEGF inhibitors and irradiation. Upon which, tumor growth was delayed for longer time and higher control for local tumor was achieved rather than either treatment alone in addition to maintaining cancer perfusion [44]. The oral treatment with the novel synthesized Pyridazino[3, 4, 5-de] quinazoline derivatives 3, 4, 5 and 6 led to an inhibition in expression of VEGFR2 in liver of irradiated rats by 42%, 55%, 48% and 66% respectively (Fig. 3), thereby identifying a potential radiosensitizing agent in liver cancer cells. It was clear from these results that the ethoxy aniline derivative 6 was the most potent VEGFR2 inhibitor showing equivalent efficacy as that of sorafenib which caused 70% inhibition of VEGFR2 (Fig. 3).

The overall mechanism of the bimodal radiation-induced VEGFR activation is currently unknown. Dent showed that the second peak of receptor activation occurs due to radiation- induced autocrine production of the VEGFR ligand, transforming growth factor alpha (TGF-α) [45]. Bridges, postulates that early radiation-induced 'activation' actually results from inhibition of intracellular phosphatases, which under normal homeostatic circumstances maintain VEGFR inactive [46]. In this study, we elucidate the possible role of a novel synthetized Pyridazino[3, 4, 5-de] quinazoline derivatives as an anti-VEGF which was induced by exposure to ionizing radiation compared to Sorafenib, one of the main monoclonal antibodies against generation of VEGF.

Apoptosis induction has become one of the approaches to drug discovery in the field of chemotherapy. Tumor pathogenesis relies on defects in the mechanisms of programmed cell death. Subsequently, neoplastic cells are allowed to survive for extended time. This is considered a self-protective effect against oxidative stress and hypoxia which occur upon increasing the tumor mass [47]. On the other hand, apoptosis and necrosis led to cell death in the normal liver [48]. As the caspase-3 activation is a common critical event for radiation induced apoptosis [49], we studied the anti-apoptotic effect of novel synthetized Pyridazino[3, 4, 5-de] quinazoline derivatives against radiation-induced apoptosis in liver of normal rats. Whole body exposure of rats to 6 Gy gamma radiation caused a remarkable apoptosis in liver tissue reflected by an elevation in caspase 3 by nearly 10 fold (Fig. 4). These results were in agreement with El-sheikh and co-workers who reported expression of caspase-3 in liver of rats after irradiation [34]. The treatment with the novel synthesized compounds 3, 4, 5 and 6 for 3 successive days after irradiation led to a decrease in caspase 3 by 67%, 61%, 74% and 83% respectively, thereby allowing the application of radiation therapy without liver damage. Ethoxy aniline derivative **6** showed nearly the same potency as that of sorafenib which decrease caspase by 85% (Fig. 4). These results are concurrent with Sonntag and co-workers who found that sorafenib specifically activates caspase-3 and apoptosis in malignant hepatoma cells but not in non-malignant hepatocytes, defining a strong tumor-specific effect of sorafenib [50]. Therefore, it might be suggested that the 4 novel synthetized Pyridazino [3, 4, 5-de] quinazoline derivatives **(3–6)**, might follow the same pattern.

5.2.3. *Toxicological study*

Furthermore, all the potent tested compounds (3, 4, 5 and 6) as VEGFR2 inhibitors, were subjected to study their acute toxicity in rats. Smith's method [36] was used to determine the approximate 50% lethal dose (ALD50) as presented in Table 2. The results revealed that the tested compounds were relatively non-toxic in experimental rats showing ALD50 > 800 mg/kg.

6. Molecular docking

Docking study was performed to predict the possible interactions of the synthesized compounds within the active binding site of VEGFR-2. Sorafenib and vatalanib were considered as reference drugs to compare their binding interactions to our compounds.

The binding pattern of sorafenib to VEGFR-2 kinase active site was found as reported with docking score (S = −17.45 kcal/mol) [51]; the 3-chloro-4-trifluoromethyphenyl group shares as a hydrophobic moiety embedded in the allosteric site. The phenyl group between urea and oxygen acts as hydrophobic moiety in the gate keeper region. On the urea linker, the core scaffold, there are two essential hydrogen bonds with Glu885 and Asp1046, in the extended channel which is located directly adjacent to the ATP binding site. Cys919 is connected by two hydrogen bonds to *N*-methylpicolinamide. Interaction with ASP1046 is

Table 2
Acute Toxicity Evaluation.

Compound no.	Acute toxicity ALD50(mg/kg bwt
Normal	–
Irradiated	–
Sorafenib	–
3	> 800
4	> 800
5	> 800
6	> 800

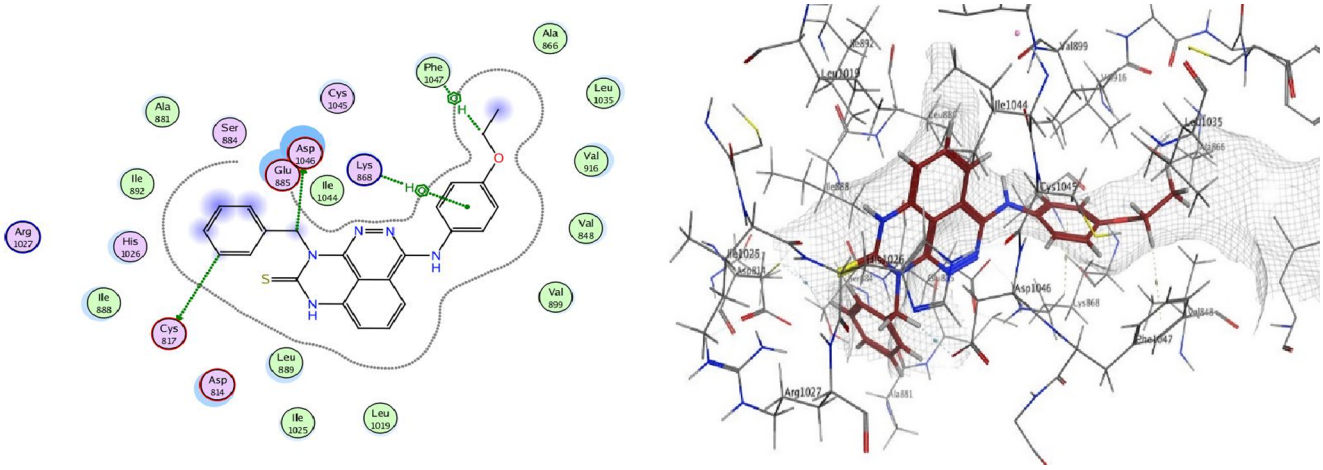

Fig. 5. 2D & 3D binding interactions of compound 6 within the active binding siteVEGFR-2 (PDB 4ASD).

required for VEGFR2 inhibition [52].

Docking of vatalanib was investigated, where it forms one hydrogen bond with Asp1046 through its pyridazine nitrogen, and with Cys919 through the chlorine atom Vatalanib also forms arene-cation interaction with Phe1047 (S = −17.12 kcal/mol). It is worth noting that binding interaction with Asp 1046 into VEGFR-2 active binding site is common among sorafenib & vatalanib (Supplementary data)

Docking simulation of the newly synthesized compounds (2-6) showed that they fit into the enzyme active binding site almost at the same positions of sorafenib and vatalanib (Supplementary data) with comparable docking scores (−15.21 to −13.12 kcal/mol) **(**Table 1**).**

It's greatly notable that the most potent ethoxy aniline derivative **6** fits into VEGRF2 enzyme active binding site through binding interaction with Lys 868 and Asp 1046 (Fig. 5) additionally, recording the best docking score energy (-15.21 Kcal/mol), among the newly synthesized compounds. It could be concluded that the ethoxy para substitution of compound **(6)** occupied a hydrophobic region within the active binding site which aids in more binding and VEGFR-2 inhibition.

7. Conclusion

The present study reported the design and synthesis of novel series of Pyridazino[3, 4, 5-de] quinazoline based on vatalanib pharmacophore as anti-VEGFR2. The synthesized compounds were evaluated for their VEGFR2 inhibitory activity compared to Sorafenib as a reference standard drug in-vitro and in-vivo. Ethoxy aniline derivative **6** was found to be as potent as Sorafenib in inhibiting VEGFR2 (IC50 = 0.03 μM). All compounds were assessed for their anti-tumor activity in-vitro, anti-apoptotic effect and toxicological studies in-vivo. Interestingly, Ethoxy aniline derivative **6** is the most potent compound in this study having antitumor activity close to that of sorafenib. Moreover, the other pyridazino quinazoline derivatives 3-5 also showed significant antitumor activity via VEGFR2 inhibition. All the tested compounds were found to be potential non-toxic to normal liver of experimental rats. The new compounds counteract the apoptotic effect induced by ionizing radiation on normal cells. Future preclinical studies will be performed on these compounds to explore a full kinase selectivity profile other than VEGFR-2 using normal cell lines and other tumor cell lines.

Declaration of Competing Interest

Authors declare that there is no conflict of interest in this work

Acknowledgement

Authors would like to express their gratitude to the staff members of gamma irradiation unit at the National Center for Radiation Research and Technology (NCRRT), for their tender cooperation in carrying out the experimental irradiation.

Appendix A. Supplementary material

Supplementary data to this article can be found online at https://doi.org/10.1016/j.bioorg.2019.103251.

References

[1] R.L. Siegel, K.D. Miller, A. Jemal, Cancer statistics, 2015, CA Cancer J. Clin. 65 (1) (2015) 5–29.
[2] D.J. Erstad, K.K. Tanabe, Hepatocellular carcinoma: early-stage management challenges, J. Hepatocell. Carcinoma 4 (2017) 81–92.
[3] L. Rimassa, HCC IN FOCUS. Current Developments in the Management of Hepatocellular Carcinoma, Gastroenterology & Hepatology, 2018, pp. 542-544.
[4] C. Guha, B.D. Kavanagh, Hepatic radiation toxicity: avoidance and amelioration, Semin. Radiat. Oncol. 21 (4) (2011) 256–263.
[5] M.A. Morse, W. Sun, R. Kim, A.R. He, P.B. Abada, M. Mynderse, R.S. Finn, The role of angiogenesis in hepatocellular carcinoma, Clin. Cancer Res. 25 (3) (2019) 912–920.
[6] H.L. Goel, A.M. Mercurio, VEGF targets the tumour cell, Nat. Rev. Cancer 13 (12) (2013) 871–882.
[7] D. Fukumura, J. Kloepper, Z. Amoozgar, D.G. Duda, R.K. Jain, Enhancing cancer immunotherapy using antiangiogenics: opportunities and challenges, Nat. Rev. Clin. Oncol. 15 (5) (2018) 325–340.
[8] J. Frayne Application of genetics, Montana publishers 2018.
[9] Y.Y. Shao, C.H. Hsu, A.L. Cheng, Predictive biomarkers of sorafenib efficacy in advanced hepatocellular carcinoma: are we getting there? World J. Gastroenterol. 21 (36) (2015) 10336–10347.
[10] K. Kim, J. Roh, H. Wee, C. Kim, Cancer drug discovery: science & history, Pan Mun Education Co., Seoul, 2015.
[11] Y. Li, Z.H. Gao, X.J. Qu, The adverse effects of sorafenib in patients with advanced cancers, Basic Clin. Pharmacol. Toxicol. 116 (3) (2015) 216–221.
[12] C. Mendez-Blanco, F. Fondevila, A. Garcia-Palomo, J. Gonzalez-Gallego, J.L. Mauriz, Sorafenib resistance in hepatocarcinoma: role of hypoxia-inducible factors, Exp. Mol. Med. 50 (10) (2018) 134.
[13] L. Pelosof, S. Lemery, S. Casak, X. Jiang, L. Rodriguez, V. Pierre, Y. Bi, J. Liu, J.F. Zirkelbach, A. Patel, K.B. Goldberg, A.E. McKee, P. Keegan, R. Pazdur, Benefit-risk summary of regorafenib for the treatment of patients with advanced hepatocellular carcinoma that has progressed on sorafenib, Oncologist 23 (4) (2018) 496–500.
[14] J. Trojan, O. Waidmann, Role of regorafenib as second-line therapy and landscape of investigational treatment options in advanced hepatocellular carcinoma, J Hepatocell Carcinoma 3 (2016) 31–36.
[15] J. Bruix, S. Qin, P. Merle, A. Granito, Y.H. Huang, G. Bodoky, M. Pracht, O. Yokosuka, O. Rosmorduc, V. Breder, R. Gerolami, G. Masi, P.J. Ross, T. Song, J.P. Bronowicki, I. Ollivier-Hourmand, M. Kudo, A.L. Cheng, J.M. Llovet, R.S. Finn, M.A. LeBerre, A. Baumhauer, G. Meinhardt, G. Han, Regorafenib for patients with hepatocellular carcinoma who progressed on sorafenib treatment (RESORCE): a randomised, double-blind, placebo-controlled, phase 3 trial, Lancet 389 (10064) (2017) 56–66.

[16] A.L. Cheng, Y.K. Kang, D.Y. Lin, J.W. Park, M. Kudo, S. Qin, H.C. Chung, X. Song, J. Xu, G. Poggi, M. Omata, S. Pitman Lowenthal, S. Lanzalone, L. Yang, M.J. Lechuga, E. Raymond, Sunitinib versus sorafenib in advanced hepatocellular cancer: results of a randomized phase III trial, J. Clin. Oncol. 31 (32) (2013) 4067–4075.
[17] J.M. Llovet, T. Decaens, J.L. Raoul, E. Boucher, M. Kudo, C. Chang, Y.K. Kang, E. Assenat, H.Y. Lim, V. Boige, P. Mathurin, L. Fartoux, D.Y. Lin, J. Bruix, R.T. Poon, M. Sherman, J.F. Blanc, R.S. Finn, W.Y. Tak, Y. Chao, R. Ezzeddine, D. Liu, I. Walters, J.W. Park, Brivanib in patients with advanced hepatocellular carcinoma who were intolerant to sorafenib or for whom sorafenib failed: results from the randomized phase III BRISK-PS study, J. Clin. Oncol. 31 (28) (2013) 3509–3516.
[18] A.X. Zhu, O. Rosmorduc, T.R. Evans, P.J. Ross, A. Santoro, F.J. Carrilho, J. Bruix, S. Qin, P.J. Thuluvath, J.M. Llovet, M.A. Leberre, M. Jensen, G. Meinhardt, Y.K. Kang, SEARCH: a phase III, randomized, double-blind, placebo-controlled trial of sorafenib plus erlotinib in patients with advanced hepatocellular carcinoma, J. Clin. Oncol. 33 (6) (2015) 559–566.
[19] L. Rimassa, E. Assenat, M. Peck-Radosavljevic, M. Pracht, V. Zagonel, P. Mathurin, E. Rota Caremoli, C. Porta, B. Daniele, L. Bolondi, V. Mazzaferro, W. Harris, N. Damjanov, D. Pastorelli, M. Reig, J. Knox, F. Negri, J. Trojan, C. Lopez Lopez, N. Personeni, T. Decaens, M. Dupuy, W. Sieghart, G. Abbadessa, B. Schwartz, M. Lamar, T. Goldberg, D. Shuster, A. Santoro, J. Bruix, Tivantinib for second-line treatment of MET-high, advanced hepatocellular carcinoma (METIV-HCC): a final analysis of a phase 3, randomised, placebo-controlled study, Lancet Oncol. 19 (5) (2018) 682–693.
[20] C. Cainap, S. Qin, W.-T. Huang, I.J. Chung, H. Pan, Y. Cheng, M. Kudo, Y.-K. Kang, P.-J. Chen, H.-C. Toh, V. Gorbunova, F.A.L.M. Eskens, J. Qian, M.D. McKee, J.L. Ricker, D.M. Carlson, S. El-Nowiem, Linifanib versus Sorafenib in patients with advanced hepatocellular carcinoma: results of a randomized phase III trial, J. Clin. Oncol Off. J. American Soc. Clin. Oncol. 33 (2) (2015) 172–179.
[21] Y. Liu, S. Zhang, Y. Li, J. Wang, Y. Song, P. Gong, Synthesis and cytotoxic evaluation of some new phthalazinylpiperazine derivatives, Arch Pharm (Weinheim) 345 (4) (2012) 287–293.
[22] E. Van Cutsem, E. Bajetta, J. Valle, C.H. Kohne, J.R. Hecht, M. Moore, C. Germond, W. Berg, B.L. Chen, T. Jalava, D. Lebwohl, G. Meinhardt, D. Laurent, E. Lin, Randomized, placebo-controlled, phase III study of oxaliplatin, fluorouracil, and leucovorin with or without PTK787/ZK 222584 in patients with previously treated metastatic colorectal adenocarcinoma, J. Clin. Oncol. 29 (15) (2011) 2004–2010.
[23] M.S. Behalo, I.A. Gad El-karim, R. Rafaat, Synthesis of novel phthalazine derivatives as potential anticancer and antioxidant agents based on 1-chloro-4-(4-phenoxyphenyl)phthalazine, J. Heterocycl. Chem. 54 (6) (2017) 3591–3599.
[24] W. Gao, C. Wang, K. Muzyka, S.A. Kitte, J. Li, W. Zhang, G. Xu, Artemisinin-luminol chemiluminescence for forensic bloodstain detection using a smart phone as a detector, Anal. Chem. 89 (11) (2017) 6160–6165.
[25] G. Vaseghi, E. Jafari, F. Hassanzadeh, S. Haghjooy-Javanmard, N. Dana, M. Rafieian-Kopaei, Cytotoxic evaluation of some fused pyridazino- and pyrroloquinazolinones derivatives on melanoma and prostate cell lines, Adv. Biomed. Res. 6 (1) (2017) 76.
[26] R.R. Radwan, N.H. Zaher, M.G. El-Gazzar, Novel 1,2,4-triazole derivatives as antitumor agents against hepatocellular carcinoma, Chem. Biol. Interact. 274 (2017) 68–79.
[27] M.G. El-Gazzar, H.M. Aly, Anticancer evaluation and docking study of new bifunctional phthalazine derivatives, Curr. Org. Synth. 15 (3) (2018) 414–422.
[28] T. Dragovich, D. Laheru, F. Dayyani, V. Bolejack, L. Smith, J. Seng, H. Burris, P. Rosen, M. Hidalgo, P. Ritch, A.F. Baker, N. Raghunand, J. Crowley, D.D. Von Hoff, Phase II trial of vatalanib in patients with advanced or metastatic pancreatic adenocarcinoma after first-line gemcitabine therapy (PCRT O4–001), Cancer Chemother. Pharmacol. 74 (2) (2014) 379–387.
[29] H. Joensuu, F. De Braud, G. Grignagni, T. De Pas, G. Spitalieri, P. Coco, C. Spreafico, S. Boselli, F. Toffalorio, P. Bono, T. Jalava, C. Kappeler, M. Aglietta, D. Laurent, P.G. Casali, Vatalanib for metastatic gastrointestinal stromal tumour (GIST) resistant to imatinib: final results of a phase II study, Br. J. Cancer 104 (11) (2011) 1686–1690.
[30] Y.M. Abdel Aziz, M.M. Said, H.A. El Shihawy, K.A. Abouzid, Discovery of novel tricyclic pyrido[3',2':4,5]thieno[3,2-d]pyrimidin-4-amine, derivatives as VEGFR-2 inhibitors, Bioorg. Chem. 60 (2015) 1–12.
[31] A. Gangjee, N. Zaware, S. Raghavan, B.C. Disch, J.E. Thorpe, A. Bastian, M.A. Ihnat, Synthesis and biological activity of 5-chloro-N(4)-substituted phenyl-9H-pyrimido [4,5-b]indole-2,4-diamines as vascular endothelial growth factor receptor-2 inhibitors and antiangiogenic agents, Bioorg. Med. Chem. 21 (7) (2013) 1857–1864.
[32] J. Cai, M. Sun, X. Wu, J. Chen, P. Wang, X. Zong, M. Ji, Design and synthesis of novel 4-benzothiazole amino quinazolines Dasatinib derivatives as potential antitumor agents, Eur. J. Med. Chem. 63 (2013) 702–712.
[33] M.M. Ghorab, M.S. Alsaid, A.M. Soliman, F.A. Ragab, VEGFR-2 inhibitors and apoptosis inducers: synthesis and molecular design of new benzo[g]quinazolin bearing benzenesulfonamide moiety, J. Enzyme Inhib. Med. Chem. 32 (1) (2017) 893–907.
[34] M.M. El-Sheikh, R.M. El-Hazek, A.S. El-Khatib, M.A. El-Ghazaly, Anti-apoptotic effect of 3-aminobenzamide, an inhibitor of poly (ADP-ribose) polymerase, against multiple organ damage induced by gamma irradiation in rats, Int. J. Radiat Biol. 94 (1) (2018) 45–53.
[35] M. Hennenberg, J. Trebicka, Z. Kohistani, C. Stark, H.D. Nischalke, B. Kramer, C. Korner, S. Klein, M. Granzow, H.P. Fischer, J. Heller, T. Sauerbruch, Hepatic and HSC-specific sorafenib effects in rats with established secondary biliary cirrhosis, Lab. Invest. 91 (2) (2011) 241–251.
[36] Q.E. Smith, Pharmacological screening test progress in medicinal chemistry, Butterworths, London, 1960.
[37] W. Sun, R. Cabrera, Systemic treatment of patients with advanced unresectable hepatocellular carcinoma: emergence of therapies, J. Gastrointestinal Cancer 49 (2) (2018) 107–115.
[38] S.B. Choi, H.J. Han, W.B. Kim, T.J. Song, S.Y. Choi, VEGF overexpression predicts poor survival in hepatocellular Carcinoma, Open Med. (Warsaw, Poland) 12 (2017) 430–439.
[39] X. Li, Y. Gao, J. Li, K. Zhang, J. Han, W. Li, Q. Hao, W. Zhang, S. Wang, C. Zeng, W. Zhang, Y. Zhang, M. Li, C. Zhang, FOXP3 inhibits angiogenesis by down-regulating VEGF in breast cancer, Cell Death Dis. 9 (7) (2018) 744.
[40] J. Wang, L. Zhang, X. Pan, B. Dai, Y. Sun, C. Li, J. Zhang, Discovery of multi-target receptor tyrosine kinase inhibitors as novel anti-angiogenesis agents, Sci. Rep. 7 (2017) 45145.
[41] H.Q. Zhuang, Z.Y. Yuan, P. Wang, Research progress on the mechanisms of combined bevacizumab and radiotherapy, Recent Pat Anticancer Drug Discov 9 (1) (2014) 129–134.
[42] H.K. Sanoff, Y. Chang, J.L. Lund, B.H. O'Neil, S.B. Dusetzina, Sorafenib effectiveness in advanced hepatocellular carcinoma, Oncologist 21 (9) (2016) 1113–1120.
[43] M. He, C. Dong, R. Ren, D. Yuan, Y. Xie, Y. Pan, C. Shao, Radiation enhances the invasiveness of irradiated and nonirradiated bystander hepatoma cells through a VEGF-MMP2 pathway initiated by p53, Radiat. Res. 180 (4) (2013) 389–397.
[44] H.J. Koo, M. Lee, J. Kim, C.W. Woo, S.Y. Jeong, E.K. Choi, N. Kim, J.S. Lee, Synergistic effect of anti-angiogenic and radiation therapy: quantitative evaluation with dynamic contrast enhanced MR imaging, PLoS ONE 11 (2) (2016) e0148784.
[45] P. Dent, MAP kinase pathways in the control of hepatocyte growth, metabolism and survival, in: J. Dufour, P. Clavien, C. Trautwein, R. Graf (Eds.), Signaling Pathways in Liver Diseases, Springer, Berlin, Heidelberg, 2005.
[46] A.J. Bridges, Chemical inhibitors of protein kinases, Chem. Rev. 101 (8) (2001) 2541–2572.
[47] M. Hassan, D. Selimovic, M. Hannig, Y. Haikel, R.T. Brodell, M. Megahed, Endoplasmic reticulum stress-mediated pathways to both apoptosis and autophagy: significance for melanoma treatment, World J. Experim. Med. 5 (4) (2015) 206–217.
[48] M.E. Guicciardi, H. Malhi, J.L. Mott, G.J. Gores, Apoptosis and necrosis in the liver, Compr. Physiol. 3 (2) (2013) 977–1010.
[49] N. Santos, R.F. Silva, M. Pinto, E.B.D. Silva, D.R. Tasat, A. Amaral, Active caspase-3 expression levels as bioindicator of individual radiosensitivity, An. Acad. Bras. Cienc. 89 (1 Suppl 0) (2017) 649–659.
[50] R. Sonntag, N. Gassler, J.M. Bangen, C. Trautwein, C. Liedtke, Pro-apoptotic Sorafenib signaling in murine hepatocytes depends on malignancy and is associated with PUMA expression in vitro and *in vivo*, Cell Death Dis. 5 (2014) e1030.
[51] S.M. Abou-Seri, W.M. Eldehna, M.M. Ali, D.A. Abou El Ella, 1-Piperazinylphthalazines as potential VEGFR-2 inhibitors and anticancer agents: Synthesis and in vitro biological evaluation, Eur. J. Med. Chem. 107 (2016) 165–179.
[52] C. Wu, M. Wang, Q. Tang, R. Luo, L. Chen, P. Zheng, W. Zhu, Design, synthesis, activity and docking study of sorafenib analogs bearing sulfonylurea unit, Molecules 20 (10) (2015) 19361–19371.